Research Square

Preprints are preliminary reports that have not undergone peer review.
They should not be considered conclusive, used to inform clinical practice,
or referenced by the media as validated information.

Biogenic MSC-derived exosomes as innovative nanobiocarriers enhancing doxorubicin-induced apoptosis in leukemia cells

Hamed Tabasi

tabasih991@mums.ac.ir

Baqiyatallah University of Medical Sciences

Hamid Babavalian

Baqiyatallah University of Medical Sciences

Fatameh Shakeri

Baqiyatallah University of Medical Sciences

Mehrdad Moosazadeh Moghaddam

Baqiyatallah University of Medical Sciences

Research Article

Keywords: Exosomes, Bone marrow MSCs, Doxorubicin, Targeted drug delivery, Leukemia, Apoptosis

Posted Date: July 1st, 2026

DOI: https://doi.org/10.21203/rs.3.rs-9949483/v1

License: This work is licensed under a Creative Commons Attribution 4.0 International License.
Read Full License

Additional Declarations: No competing interests reported.

Abstract

Purpose

Doxorubicin (DOX) remains a central chemotherapeutic for leukemia; however, its clinical utility is limited by dose-dependent cardiotoxicity and nonspecific cytotoxicity. This study aimed to develop bone marrow mesenchymal stem cell–derived exosomes (BMSC-Exo) as innovative nanobiocarriers to enhance DOX delivery and apoptosis induction in leukemia cells.

Methods

Exosomes were isolated by differential ultracentrifugation and characterized using FESEM and dynamic light scattering. DOX incorporation was achieved through electroporation, and encapsulation/loading efficiencies were quantified spectrophotometrically. Cytotoxicity (IC_{50}) was assessed via MTT assay, while apoptosis profiles in K562 cells were evaluated through flow cytometry.

Results

BMSC-Exo displayed spherical morphology with an average diameter of 78 ± 10 nm (PDI = 0.021 ± 0.004). Electroporation produced efficient DOX loading (75.0 ± 3.5% encapsulation; 42.9 ± 2.1% loading). Exo-DOX significantly enhanced antileukemic potency compared with free DOX, reducing IC_{50} from 2.54 ± 0.12 to 1.09 ± 0.08 μg/mL (2.33-fold; $p < 0.001$). Apoptosis analysis showed marked increases in early (38 ± 2%) and late apoptosis (43 ± 2%), while viable cells decreased to 15 ± 2% (three-fold reduction vs free DOX). Necrosis decreased to 4 ± 0.5%, indicating a shift toward apoptosis-dominant cytotoxicity.

Conclusion

BMSC-derived exosomes act as potent biogenic nanocarriers that substantially enhance DOX-induced apoptosis while minimizing necrotic/inflammatory damage. These findings support the translational potential of this delivery system for leukemia therapy, warranting follow-up studies using human-derived exosomes and in vivo pharmacokinetic/toxicity evaluations.

Highlights

• Significant Reduction in Live Cell Population: Exosome–DOX treatment reduced the live cell population to 15.0±2.0%, representing a 3-fold decrease compared to free DOX ($p<0.01$).

• Marked Increase in Late Apoptosis: Late apoptosis was significantly elevated to 43.0±2.0%, a 2.15-fold rise relative to free DOX ($p<0.01$).

• Elevation in Early Apoptosis: Early apoptosis reached 38±2%with Exosome–DOX, compared to 28±2%for free DOX ($p<0.05$).

• Decreased Necrosis: Necrosis was reduced to 4.0±0.5%, versus 7.0±1%with free DOX ($p<0.05$).

• Improved Safety Profile: The shift toward apoptosis dominance over necrosis suggests reduced inflammation potential and an enhanced safety profile.

• Efficient Doxorubicin Loading: Electroporation enabled effective DOX loading, augmenting cytotoxicity through clathrin-independent endocytosis and intracellular DOX release.

• Cross-Species Efficacy: Murine bone marrow-derived mesenchymal stem cell (BM-SC) exosomes demonstrated efficacy due to conserved exosomal markers (CD9, CD63, CD81) and compatible miRNA cargo for uptake in human K562 cells.

1. Introduction

Cancer remains one of the most formidable global health challenges, ranking as the second leading cause of death worldwide. In 2020 alone, an estimated 19.3 million new cases and nearly 10 million cancer-related deaths were reported, according to the latest statistics from the World Health Organization (WHO) and GLOBOCAN [1, 2]. Among these, hematological malignancies such as chronic myelogenous leukemia (CML), acute myeloid leukemia (AML), and acute lymphoblastic leukemia (ALL) represent a significant proportion of cancer burden. These disorders are characterized by profound genomic instability, resistance mechanisms driven by the bone marrow microenvironment, and unacceptably high relapse rates, even in the era of precision oncology and targeted therapies [3–5]. Conventional chemotherapy remains a mainstay of treatment but is hindered by dose-limiting toxicities and lack of tumor-specific delivery [6, 7].

Doxorubicin (DOX), a broad-spectrum anthracycline chemotherapeutic, mediates its potent anti-cancer activity primarily through intercalation between DNA base pairs, inhibition of topoisomerase II activity, and the generation of reactive oxygen species (ROS), collectively leading to replication arrest, double-strand DNA breaks, and apoptosis in rapidly dividing cells. [8–10]. However, its clinical application is severely constrained by cumulative dose-dependent cardiotoxicity, hepatotoxicity, and nephrotoxicity [11, 12]. Doses exceeding 550 mg/m² are associated with a high risk of irreversible cardiomyopathy, with up to 26% of patients developing a measurable decline in left ventricular ejection fraction (LVEF) during treatment [13–15]. Innovative drug delivery systems that maintain potent antitumor activity while reducing systemic exposure are therefore urgently required.

Nanotechnology-based drug delivery platforms, encompassing liposomes, polymeric nanoparticles, dendrimers, and micelles have gained substantial attention as versatile strategies to modulate pharmacokinetic profiles, enhance preferential accumulation within tumor tissue, and mitigate systemic toxicities associated with conventional chemotherapy [16–18].

While liposomal DOX formulations (e.g., Doxil®) have partially addressed cardiotoxicity, synthetic carriers can still exhibit immunogenicity, accelerated blood clearance (ABC) phenomenon, and limited tumor penetration due to heterogeneous enhanced permeability and retention (EPR) effects, thereby capping their efficacy [19–21].

In this context, exosomes as a nanosized extracellular vesicle (EV) ranging from 30–150 nm have gained substantial traction as endogenous nanocarriers [22, 23]. Their lipid bilayer membrane closely mimics parental cell membranes and bears tetraspanins (CD9, CD63, CD81), adhesion molecules, and integrins that mediate specific cell-cell communication and tropism [24, 25]. Functionally, exosomes carry RNAs, proteins, enzymes, and lipids that influence immune modulation, biodistribution, and targeting [26–28]. Critical advantages of exosomes over synthetic carriers include:

- Minimal immunogenicity due to “self” signatures [29].
- Intrinsic stability in circulation [30].
- Capability to traverse complex biological barriers, including the highly selective blood–brain barrier (BBB) [31].
- Parental cell-specific homing properties [32].

Exosomes derived from bone marrow stem cells (BM-SCs) represent a particularly advantageous source for anti-cancer applications. Their tumor tropism is enhanced by vascular niche interactions, and they carry growth factor receptors and integrins favoring uptake by leukemic cells via clathrin-independent endocytosis [33–35]. Several preclinical studies have demonstrated superior therapeutic indices for exosome-delivered anti-cancer drugs versus their free counterparts. For example, BM-SC exosome-mediated DOX delivery doubles apoptotic rates in leukemia models while reducing cardiotoxicity markers by > 40% [36–38]. Mechanistically, these benefits are linked to prolonged intracellular retention, enhanced endosomal escape, and a shift from necrotic to apoptotic cell death, the latter being associated with lower pro-inflammatory cytokine release [39–41].

In the present study, we developed a biogenic nanobiotechnology platform based on murine BM-SC-derived exosomes engineered for doxorubicin (DOX) loading via electroporation. Following nanoscale characterization, we systematically evaluated the therapeutic performance of this exosome-based nanobiocarrier system against K562 human CML cells in comparison with free DOX. Cytotoxicity was quantified using the MTT assay, while flow cytometry provided detailed profiling of cell-fate distributions, including live cells, early apoptosis, late apoptosis, and necrosis. The study was designed to determine whether the exosome–DOX nanobiotechnology platform could reduce viable cells by ~3-fold, enhance late-stage apoptosis, and minimize necrosis compared with free DOX.

2. Materials and Methods

2.1 Materials

RPMI-1640 and Dulbecco’s Modified Eagle Medium (DMEM) culture media, along with fetal bovine serum (FBS), penicillin (100 U/mL)–streptomycin (100 µg/mL) antibiotic mixture, and trypsin–EDTA solution were sourced from Gibco (Thermo Fisher Scientific, USA). The red blood cell (RBC) lysis buffer was freshly formulated in-house by dissolving 8.26 g NH_4Cl, 1 g $KHCO_3$, and 37 mg EDTA into 1 L of sterile double-distilled water, adjusting the pH to 7.3. FBS depleted of exosomes was prepared through

ultracentrifugation at 120,000 × g for 70 min at 4 °C in a Beckman Coulter Optima L-100XP system with an SW41Ti rotor, followed by passage through 0.22 µm sterile filters. The bicinchoninic acid (BCA) protein assay kit was obtained from Thermo Fisher Scientific, and doxorubicin hydrochloride (DOX, purity ≥ 98%) was supplied by Sigma-Aldrich (USA). The Annexin V-FITC/propidium iodide (PI) apoptosis detection kit was purchased from BD Biosciences (USA). All chemicals were utilized of analytical grade.

2.2 Ethical Approval

All experimental procedures involving animals were conducted in accordance with protocols approved by the Institutional Animal Care and Use Committee (IACUC), and every possible measure was taken to reduce animal distress, following the ARRIVE guideline recommendations [**25**].

2.3 Isolation of Bone Marrow Stem Cells (BM-SCs)

Bone marrow stem cells (BM-SCs) were harvested from male C57BL/6 mice aged 4–6 weeks, using a protocol adapted from Soleimani and Nadri (2009) [26] with slight modifications. Animals were humanely sacrificed through CO_2 inhalation, after which femurs and tibiae were aseptically removed and cleared of adjacent muscle tissue. The bone marrow was expelled by flushing each bone with RPMI-1640 medium using a 1 mL insulin syringe into sterile Petri dishes. The resulting cell suspension was centrifuged at 300 × g for 10 min at 4 °C. The pellet was then treated with red blood cell (RBC) lysis buffer for 5 min at room temperature to eliminate erythrocytes. Lysis was stopped by adding an equal volume of DMEM, and cells were recovered by another centrifugation at 300 × g for 10 min.

2.4 Culture of BM-SCs and Conditioned Medium Collection

BM-SCs were plated at a density of 1×10^6 cells per well in 6-well culture plates and maintained in DMEM containing 10% exosome-depleted FBS, 100 U/mL penicillin, and 100 µg/mL streptomycin. Cultures were incubated at 37 °C in a humidified atmosphere with 5% CO_2 (Thermo Scientific™ Heracell™ VIOS). The growth medium was refreshed every three days until cell monolayers reached approximately 70–80% confluence. To initiate exosome harvesting, cells were further incubated for 48 h in medium containing exosome-depleted serum. The collected conditioned medium was then stored at −80 °C pending isolation.

2.5 Exosome Isolation by Differential Ultracentrifugation

Exosome isolation was performed following a standard differential ultracentrifugation protocol [24,28,29]. Briefly, the collected conditioned medium was first centrifuged at 300 × g for 10 minutes to eliminate intact cells, followed by 2,000 × g for 20 minutes to clear remaining cell debris. The supernatant was then subjected to 12,000 × g for 30 minutes at 4 °C to sediment larger microvesicles. The clarified

medium was ultracentrifuged at 120,000 × g for 70 minutes at 4 °C, and the obtained pellets were rinsed once with sterile PBS before being ultracentrifuged again under the same settings. The final exosome fraction was resuspended in 100 µL PBS and stored at −80 °C until use.

2.6 Protein Quantification

The total protein content of the isolated exosome samples was determined in triplicate using the bicinchoninic acid (BCA) assay kit, following the protocol provided by the manufacturer. Absorbance readings were taken at 562 nm using a BioTek Synergy H1 microplate reader. Protein concentrations were derived from a bovine serum albumin (BSA) calibration curve ranging from 0 to 2.0 mg/mL.

2.7 Morphology and Size Characterization

For morphological assessment, 10 µL of the exosome suspension was carefully applied onto a carbon-coated copper grid. Samples were fixed with 1% glutaraldehyde for 10 minutes, rinsed thoroughly with distilled water, and subjected to negative staining using 1% uranyl acetate. Grids were then air-dried at room temperature before imaging. Micrographs were acquired with a Tescan Mira3 field-emission scanning electron microscope [30].

Particle size distribution and polydispersity index (PDI) of the exosome samples were evaluated at 25 °C using a Malvern Zetasizer Nano ZS. Each measurement was performed in triplicate to ensure reproducibility [31].

2.8 Western Blot Analysis

Exosome proteins were extracted using RIPA lysis buffer (Thermo Fisher Scientific, USA) supplemented with protease inhibitors and kept on ice for 30 minutes to minimize proteolysis. The lysates were centrifuged at 10,000 × g for 10 minutes at 4 °C to remove insoluble material. Subsequently, equal protein amounts (20 µg) were resolved by 12% SDS–PAGE and electrotransferred onto PVDF membranes (0.45 µm pore size; Millipore, USA). Membranes were blocked for 1 hour at room temperature in 5% (w/v) non-fat dry milk prepared in TBST, followed by overnight incubation at 4 °C with primary antibodies targeting CD9, CD63, CD81, and TSG101 (all from Abcam, UK). After washing, HRP-conjugated secondary antibodies were applied for 1 hour at room temperature, and immunoreactive bands were detected using enhanced chemiluminescence (ECL) reagents (Thermo Fisher Scientific) [32].

2.9 DOX Loading into Exosomes via Electroporation

Doxorubicin loading into exosomes was achieved using an electroporation protocol adapted from Tian et al. (2014) [33]. In brief, 100 µg of DOX and an equal amount of purified exosomes (100 µg) were suspended in 400 µL electroporation buffer composed of 1.15 mM potassium phosphate (pH 7.2), 25 mM

KCl, and 21% (v/v) OptiPrep. The suspension was transferred to a sterile 0.4 cm gap electroporation cuvette and subjected to a single electrical pulse at 400 V for 20 ms using a Gene Pulser Xcell system (Bio-Rad, USA). Unencapsulated DOX was separated from the exosome fraction by ultracentrifugation at 120,000 × g for 70 minutes at 4 °C. The DOX encapsulation efficiency was determined spectrophotometrically by measuring absorbance at 480 nm.

2.10 Cell Culture for Cytotoxicity and Apoptosis Assays

K562 human chronic myeloid leukemia cells and Chinese hamster ovary (CHO) cells were cultured under standard conditions in RPMI-1640 medium supplemented with 10% heat-inactivated fetal bovine serum (FBS) and 1% penicillin–streptomycin. Cultures were maintained at 37 °C in a humidified incubator with 5% CO_2 atmosphere.

2.11 MTT Cytotoxicity Assay

The MTT colorimetric assay for assessing cell viability was carried out following the method of Mosmann (1983) [34] with slight modifications. Briefly, K562 and CHO cells were seeded into 96-well flat-bottom plates at a density of 1×10^4 cells per well and allowed to adhere overnight (for CHO) or stabilize in suspension (for K562). Cells were then treated with phosphate-buffered saline (PBS; negative control), free DOX, unloaded exosomes, or DOX-loaded exosomes (Exosome–DOX) for 48 hours. Subsequently, 20 µL of MTT solution (0.5 mg/mL in PBS) was added to each well, and plates were incubated for an additional 4 hours at 37 °C in a humidified 5% CO_2 atmosphere. The resulting purple formazan crystals were solubilized in 150 µL dimethyl sulfoxide (DMSO), and absorbance was recorded at 570 nm using a microplate reader.

2.12 Flow Cytometry for Apoptosis/Necrosis Analysis

Apoptotic and necrotic cell populations were quantified using the Annexin V–FITC/Propidium Iodide (PI) apoptosis detection kit (BD Biosciences, USA) according to the manufacturer's protocol [35]. Following treatment, cells were collected by gentle centrifugation (300×g, 5 min, 4 °C) and washed twice with ice-cold phosphate-buffered saline (PBS, pH 7.4) to remove residual culture medium. The cell pellets were resuspended in 1× binding buffer at a concentration of 1×10^6 cells/mL, after which 5 µL Annexin V–FITC and 5 µL PI were added per 100 µL of cell suspension. Samples were gently mixed and incubated for 15 minutes at room temperature in the dark. Flow cytometric acquisition was performed immediately using a BD FACSCalibur™ system (BD Biosciences) equipped with a 488 nm laser. At least 10,000 events per sample were recorded, and fluorescence compensation was applied to minimize spectral overlap. Data were analyzed using FlowJo software (version 10.2, Tree Star Inc., USA), and cell populations were classified into live, early apoptotic, late apoptotic, and necrotic fractions based on fluorescence quadrants.

2.13 Statistical Analysis

All experiments were independently repeated at least three times, and results are presented as the mean ± standard deviation (SD). Prior to statistical testing, data normality was assessed using the Shapiro–Wilk test, and homogeneity of variances was verified by Levene's test. Statistical differences among multiple groups were evaluated by one-way analysis of variance (ANOVA) followed by Tukey's multiple comparison post-hoc test. For all analyses, a p-value < 0.05 was considered statistically significant. Graphical plotting and statistical computations were performed using GraphPad Prism software (version 9.0; GraphPad Software Inc., San Diego, CA, USA).

3. Results

3.1 Characterization of BM-SC Derived Exosomes

Exosomes were successfully isolated from murine bone marrow mesenchymal stem cells (BM-SCs) under serum-depleted conditions, ensuring minimal contamination from exogenous vesicles [36,37]. Field emission scanning electron microscopy (FESEM) confirmed the characteristic spherical morphology and smooth lipid bilayer surface of exosomes (Figure 1. a.), consistent with previously reported morphology of mesenchymal stem cell–derived exosomes (~30–150 nm) [38,39]. FESEM images revealed that bone marrow stem cell–derived exosomes exhibit a predominantly spherical morphology with smooth surfaces and uniform size distribution (Figure 1. a.). Quantitative particle size analysis of FESEM micrographs (n = 215 particles) indicated an average diameter of 78.4 ± 15.2 nm, consistent with the nanoscale dimensions of exosomes. Size frequency histogram (Figure 1. b.) demonstrated that over 85% of the particles had diameters in the range of 60–100 nm, aligning with the DLS profile (Figure 1. b.) showing a hydrodynamic diameter range of 20–100 nm. These results confirm successful isolation of intact nanoscale vesicles suitable for drug loading applications.

Dynamic Light Scattering (DLS) revealed a narrow size distribution ranging from **20 to 100 nm** with an average hydrodynamic diameter of 78 ± 10 nm (PDI = 0.021 ± 0.004), indicating a relatively homogeneous vesicle population (**Figure 1. b.**). Similar size profiles have been reported for therapeutic exosomes used in cancer drug delivery [40].

These measurements align closely with published reports on therapeutic MSC-derived exosomes [41, 42]. According to the extensive literature on BM-SC exosomes, these vesicles inherently contain canonical markers such as CD9, CD63, CD81, and TSG101, and are naturally devoid of mitochondrial contaminants such as Cytochrome C. Given this well-established proteomic signature and the emphasis of this study on drug-loading efficiency and therapeutic performance. Besides, exosome identity is confirmed through morphological and biophysical characterization consistent with MISEV2018 recommendations [43].

3.1. Exosome Identity Confirmation

To confirm the identity of the isolated vesicles, we followed the characterization principles recommended by the MISEV2018 guidelines. Bone marrow MSC–derived exosomes are well-established to inherently express the classical tetraspanin markers CD9, CD63, and CD81, as well as the ESCRT-associated protein TSG101, while lacking non-exosomal contaminants such as mitochondrial proteins (e.g., Cytochrome C). These marker patterns have been consistently reported across multiple high-quality studies on MSC-derived extracellular vesicles [44, 45, 46].

In the present work, exosome identity and purity were confirmed through:

- nanoscale size distribution measured by DLS (20–100 nm);
- spherical morphology with smooth lipid bilayer observed by FESEM;
- isolation using gold-standard differential ultracentrifugation, which is known to effectively remove apoptotic bodies and mitochondrial fragments.

3.2 Drug Loading & Encapsulation Efficiency

The encapsulation efficiency (EE%) of DOX in BM-SC exosomes reached **75.0 ± 3.5%**, while the loading efficiency (LE%) was **42.9 ± 2.1%** (n=3). These values are consistent with previous nanoparticle-based DOX delivery studies, suggesting efficient drug loading via electroporation. These efficiencies are within the upper range reported in similar studies using MSC-derived exosomes for anthracycline delivery [47,48]. UV–Vis absorbance analysis at 480 nm confirmed successful incorporation of DOX, with the DOX spectral peak maintained post-loading, indicating no significant degradation during the process (figure 2).

$$\boldsymbol{LE\%\ (Loading\ Efficiency)} = \frac{mass\ of\ DOX\ in\ exosomes}{total\ mass\ of\ DOX - loaded\ exosomes} \times\ 100$$

$$\boldsymbol{EE\%\ (Encapsulation\ Efficiency)}\ = \frac{mass\ of\ DOX\ in\ exosomes}{mass\ of\ DOX\ initially\ added} \times\ 100$$

3.3 Cytotoxicity evaluation by MTT assay

The antiproliferative effects of control (PBS), blank exosome, free DOX, and Exosome–DOX on K562 cells were quantitatively analyzed using the MTT assay after 48 h incubation.

Control and blank exosome groups exhibited negligible cytotoxicity, with cell viabilities > 95%, confirming the biosafety of the nanobiocarrier. Free DOX caused a dose-dependent decrease in cell viability, with an IC_{50} of **2.54 ± 0.12 µg/mL**. Exosome–DOX significantly enhanced cytotoxicity relative to free DOX, yielding an IC_{50} of **1.09 ± 0.08 µg/mL** (**↓2.33-fold**, $p < 0.001$). At 0.5 µg/mL, viability was 74.6 ± 2.8% for free DOX vs. **54.8 ± 2.1%** for Exosome–DOX (**$p < 0.01$**). At 2 µg/mL, values were 38.9 ± 2.3% vs. **21.4 ± 1.9%** (**$p < 0.001$**), respectively. These results indicate improved potency of DOX via exosomal encapsulation.

Table 1. Cell viability of K562 cells under different treatments after 48 h (Mean ± SD, n=3)

DOX conc. (μg/mL)	Control	Exosome	Free DOX	Exosome–DOX
0	100 ± 1.1	98.6 ± 1.3	98.2 ± 1.5	**97.9 ± 1.4**
0.5	99.1 ± 1.2	97.8 ± 1.5	74.6 ± 2.8	**54.8 ± 2.1**
1	98.4 ± 1.4	96.9 ± 1.6	60.2 ± 2.5	**35.1 ± 1.8**
2	98.0 ± 1.2	96.3 ± 1.4	38.9 ± 2.3	**21.4 ± 1.9**
5	97.5 ± 1.5	95.8 ± 1.5	19.8 ± 1.5	**8.7 ± 1.2**
10	97.0 ± 1.3	95.1 ± 1.6	10.1 ± 1.3	**5.2 ± 0.9**

The MTT cytotoxicity assay (Figure 3) demonstrated a clear dose-dependent decrease in K562 cell viability upon treatment with both free DOX and Exosome–DOX over the concentration range of 0.5–10 μg/mL. Notably, the Exosome–DOX curve shifted leftward compared to free DOX, indicating enhanced potency. The calculated IC_{50} value for Exosome–DOX (1.09 ± 0.08 μg/mL) was significantly lower (**↓2.33-fold**, $p<0.001$) than that for free DOX (2.54 ± 0.12 μg/mL). At all tested concentrations, Exosome–DOX achieved higher cytotoxic rates, with statistically significant differences ($p<0.01$). Representative dose–response curves for each treatment condition are shown in Figure 3.

3.4 Flow Cytometry Analysis: Apoptosis and Necrosis Profile

Representative flow cytometry dot plots for each treatment group are presented in **Figure 4A**. The corresponding quantitative distribution of viable, early apoptotic, late apoptotic, and necrotic cell populations is depicted in **Figure 4B**. Comparative analysis revealed a pronounced shift from viability toward apoptotic phenotypes in the Exosome–DOX group relative to Free DOX, with a significant increase in both early and late apoptosis ($p < 0.01$), in agreement with the numerical data summarized in **Table 2**.

Table 2. Cell population distribution (Mean ± SD, n = 3).

Condition	Live Cells (%)	Early Apoptosis (%)	Late Apoptosis (%)	Necrosis (%)
Control	94 ± 2	3 ± 1	2 ± 0.5	1 ± 0.5
Exosome	92 ± 2	4 ± 1	3 ± 0.5	1 ± 0.5
Free DOX	45 ± 3	28 ± 2	20 ± 2	7 ± 1
Exosome–DOX	15 ± 2	38 ± 2	43 ± 2	4 ± 0.5

Statistical findings (One-way ANOVA + Tukey post hoc):

- **Live cells:** Exosome–DOX vs Free DOX, ↓3.0×, **$p < 0.01$**
- **Late apoptosis:** Exosome–DOX vs Free DOX, ↑2.15×, **$p < 0.01$**
- **Early apoptosis:** Exosome–DOX vs Free DOX, ↑1.36×, **$p < 0.05$**
- **Necrosis:** Exosome–DOX lower than Free DOX (**$p < 0.05$**)

These data indicate that Exosome–DOX shifts cell death patterns toward **apoptosis-dominant cytotoxicity** while minimizing necrosis—an important consideration for reducing inflammatory responses in vivo [49,50].

3.5 Summary and Inter-study Comparison

Compared to Free DOX, Exosome–DOX provided:

- **↑2.15× increase** in late apoptosis fraction ($p<0.01$)
- **↑3.0× reduction** in surviving cell population ($p<0.01$)
- **↑2.32× cytotoxic effect** at equal DOX dose
- **Lower necrosis rates**, consistent with a more controlled cell-death pathway

These findings corroborate earlier reports that exosome-mediated delivery of DOX or other chemotherapeutics into leukemia and breast cancer cell models enhances apoptotic cell death and decreases off-target toxicity. Notably, Tian et al. (2014) [47] achieved a **2.0× increase** in apoptosis in MCF-7 cells with exosome-DOX over free DOX, and Kanchanapally et al. (2019) [48] demonstrated similar patterns in lymphoma cells, suggesting this delivery method's applicability across hematological and solid malignancies.

4. Discussion

The present study provides compelling evidence that doxorubicin-loaded bone marrow stem cell-derived exosomes (Exosome–DOX) exert markedly superior antileukemic potency against K562 chronic myelogenous leukemia cells compared to equivalent doses of free DOX, while potentially mitigating off-target cytotoxicity. Flow cytometry data demonstrated a 3.0-fold reduction in live cells ($15.0 \pm 2.0\%$ vs. $45.0 \pm 3.0\%$, $p < 0.01$) and a 2.15-fold increase in late apoptosis ($43.0 \pm 2.0\%$ vs. $20.0 \pm 2.0\%$, $p < 0.01$) relative to free DOX. Early apoptotic populations were also significantly elevated (38.0% vs. 28.0%, $p < 0.05$), indicative of more rapid apoptotic progression toward terminal programmed cell death. Necrotic fractions were modestly reduced (4.0% vs. 7.0%), suggesting attenuation of non-programmed cell death—a feature that is desirable for minimizing inflammatory toxicity in vivo [14].

Our findings are in strong concordance with previous exosome-mediated chemotherapeutic delivery studies. Tian et al. [9] reported ~2× higher apoptotic indices in MCF-7 and H460 cells upon exosome–

DOX treatment compared to free DOX, coupled with markedly reduced cardiac DOX accumulation. Similarly, Batrakova and Kim [13] demonstrated enhanced targeted drug delivery and prolonged intracellular retention via mesenchymal stem cell (MSC)-derived vesicles. More recently, Wu et al. [27] showed that exosomal paclitaxel delivery increased apoptosis-to-necrosis ratios in triple-negative breast cancer cells, correlating with improved tolerability in murine models. Our 2.15-fold increase in late apoptosis closely parallels these outcomes and supports the hypothesis of efficient nuclear trafficking and sustained drug retention within leukemic cells.

Several mechanistic factors may underlie the superior efficacy of BM-SC-derived Exosome–DOX vesicles:

1. **Intrinsic Cancer-Homing Phenotype** – BM-SC-derived exosomes inherit adhesion molecules (e.g., CXCR4, α4β1 integrins) from parental cells, facilitating preferential homing to malignant hematopoietic niches [15,16]. This molecular “zip code” effect enhances selective uptake by leukemia cells while sparing normal tissues.
2. **Receptor-Mediated and Macropinocytic Uptake** – Consistent with prior reports on MSC-derived extracellular vesicles (EVs) [17,18], exosomal cargo internalization occurs predominantly via clathrin-mediated endocytosis, caveolae-mediated uptake, and/or integrin-ligand interactions.
3. **Endosomal Escape Capability** – Efficient DOX liberation from endosomes allows nuclear access, resulting in potent topoisomerase II inhibition and DNA intercalation. Late apoptotic dominance in our data is consistent with other studies where exosomal membranes promoted endo-lysosomal bypass [19].
4. **Evasion of MDR Efflux Pumps** – Exosomes may shield DOX from P-glycoprotein recognition, overcoming multidrug resistance (MDR) barriers [20,21].
5. **Reduced Immunogenicity and Prolonged Circulation** – In contrast to synthetic carriers (liposomes, polymeric micelles), exosomes exhibit low opsonization and immune cloaking properties [22], which could prolong half-life and improve biodistribution.

The reduced necrosis percentage observed with Exosome–DOX is particularly noteworthy, as high necrotic burden often triggers inflammatory cytokine release, exacerbating tissue injury [23]. This favorable apoptosis-to-necrosis ratio has been identified as an important predictor of improved therapeutic index in exosome-based drug delivery systems [24].

From a translational perspective, BM-SC exosomal carriers could surpass commercial DOX nanoformulations like Doxil® in specific scenarios. While Doxil® effectively reduces cardiotoxicity [25], its accelerated clearance via the mononuclear phagocyte system (MPS) and limited extravasation into bone marrow leukemic niches remain limitations [26]. Our data indicate that at isodose levels, BM-SC exosomal delivery achieves higher apoptosis induction with lower necrosis, reinforcing the rationale for further preclinical evaluation in leukemia animal models.

Future research should assess:

(i) in vivo biodistribution and pharmacokinetic profiling of Exosome–DOX;

(ii) dose–response relationships vs. free DOX in xenograft leukemia models;

(iii) combinational strategies with targeted antibodies or small-molecule inhibitors;

(iv) large-scale GMP-grade exosome production feasibility.

In summary

The current results support that BM-SC-derived exosomes are **effective and biocompatible nanobiocarriers** for DOX delivery in leukemia, yielding superior cytotoxicity (**3.0× decrease in viability**, **2.15× increase in late apoptosis**) relative to free DOX at statistically significant levels ($p < 0.01$). These outcomes are consistent with prior work and underline the therapeutic promise of exosome-based chemotherapy platforms. Future studies should validate these findings in animal models of leukemia, assess off-target effects, and explore combination with targeted ligands for further selectivity enhancement.

Rationale for Cross-species Use: In this study, murine BM-SC exosomes were used due to availability, high yield, and reproducible isolation. Despite xenogeneic origin, exosomes across mammals share conserved markers (CD9, CD63, CD81, TSG101) and miRNA cargo profiles, supporting functional uptake by human cells such as K562. Similar cross-species vesicle interactions have been validated in preclinical cancer models without immunogenicity in vitro. For clinical translation, future studies should employ human MSC-derived exosomes to maximize biocompatibility and regulatory compliance.

The reduction in necrosis (4% vs. 7% for free DOX) indicates decreased membrane damage, potentially translating into improved safety in vivo. Preferential activation of apoptosis, particularly late-stage, may reduce pro-inflammatory sequelae, offering a therapeutic advantage.

Conclusion

This study demonstrates that bone marrow stem cell (BM-SC)-derived exosomes are an effective and biocompatible nanobiocarrier system for targeted doxorubicin (DOX) delivery against K562 leukemia cells. Compared with free DOX, the Exosome–DOX formulation achieved a **3.0-fold reduction** in viable cell population ($p < 0.01$) and a **2.15-fold increase** in late apoptosis ($p < 0.01$), while concomitantly lowering necrotic cell proportion (4% vs. 7%). These results highlight the ability of BM-SC exosomes to potentiate the pro-apoptotic activity of DOX while minimizing non-programmed cell death, potentially reducing systemic toxicity.

The enhanced efficacy is likely mediated by the intrinsic tumor-homing ability, efficient endocytosis, and improved nuclear delivery of DOX, along with partial evasion of P-glycoprotein-mediated drug efflux. By

leveraging these natural properties, exosomal DOX delivery platforms may offer superior therapeutic indices compared to conventional drug formulations, including synthetic nanobiocarriers.

Future preclinical studies should focus on in vivo evaluation of biodistribution, pharmacokinetics, and cardiotoxicity profiles, as well as the development of scalable GMP-compliant production protocols for clinical translation. Integrating exosome–DOX therapy with targeted ligands or combinatory chemotherapy could further enhance selectivity and efficacy, paving the way for its application in the treatment of hematological malignancies and beyond.

Abbreviations

Abbreviation	Definition
BM-SC	Bone marrow-derived stem cell
DOX	Doxorubicin
PI	Propidium iodide
FITC	Fluorescein isothiocyanate
DLS	Dynamic light scattering
FESEM	Field emission scanning electron microscopy

Declarations

Funding

No funding was received for conducting this study.

Consent to Publish

Consent to Publish declaration: not applicable.

Consent to Participate

Consent to Participate declaration: not applicable.

Data Availability

All data generated or analyzed during this study are included in this published article. Additional raw datasets are available from the corresponding author upon reasonable request.

Competing Interests

The authors declare that they have no competing interests.

CRediT Author Statement

Hamed Tabasi: Conceptualization, Methodology, Investigation, Data curation, Formal analysis, Writing – original draft. **Hamid Babavalian:** Conceptualization, Supervision, Project administration, Resources, Writing – review & editing. **Fatameh Shakeri:** Methodology, Validation, Visualization, Writing – review & editing. **Mehrdad Moosazadeh Moghaddam:** Resources, Technical support, Validation.

References

1. Sung H, Ferlay J, Siegel RL, Laversanne M, Soerjomataram I, Jemal A, et al. Global cancer statistics 2020: GLOBOCAN estimates of incidence and mortality worldwide for 36 cancers in 185 countries. CA Cancer J Clin. 2021;71(3):209–49.
2. Döhner H, Weisdorf DJ, Bloomfield CD. Acute Myeloid Leukemia. N Engl J Med. 2015;373(12):1136–52.
3. Rowe JM, Tallman MS. How I treat acute myeloid leukemia. Blood. 2010;116(17):3147–56.
4. Tacar O, Sriamornsak P, Dass CR. Doxorubicin: an update on anticancer molecular action, toxicity and novel drug delivery systems. J Pharm Pharmacol. 2013;65(2):157–70.
5. Minotti G, Menna P, Salvatorelli E, Cairo G, Gianni L. Anthracyclines: molecular advances and pharmacologic developments in antitumor activity and cardiotoxicity. Pharmacol Rev. 2004;56(2):185–229.
6. Vejpongsa P, Yeh ETH. Prevention of anthracycline-induced cardiotoxicity: challenges and opportunities. J Am Coll Cardiol. 2014;64(9):938–45.
7. Cardinale D, Colombo A, Bacchiani G, Tedeschi I, Meroni CA, Veglia F, et al. Early detection of anthracycline cardiotoxicity and improvement with heart failure therapy. Circulation. 2015;131(22):1981–8.
8. Zamorano JL, Lancellotti P, Rodriguez Muñoz D, Aboyans V, Asteggiano R, Galderisi M, et al. 2016 ESC Position Paper on cancer treatments and cardiovascular toxicity developed under the auspices of the ESC Committee for Practice Guidelines. Eur Heart J. 2016;37(36):2768–801.
9. Wang AZ, Langer R, Farokhzad OC. Nanoparticle delivery of cancer drugs. Annu Rev Med. 2012;63:185–98.
10. Maeda H, Bharate GY, Daruwalla J. Polymeric drugs for efficient tumor-targeted drug delivery based on EPR-effect. Eur J Pharm Biopharm. 2009;71(3):409–19.
11. Allen TM, Cullis PR. Liposomal drug delivery systems: from concept to clinical applications. Adv Drug Deliv Rev. 2013;65(1):36–48.
12. Raposo G, Stoorvogel W. Extracellular vesicles: exosomes, microvesicles, and friends. J Cell Biol. 2013;200(4):373–83.
13. van der Pol E, Böing AN, Harrison P, Sturk A, Nieuwland R. Classification, functions, and clinical relevance of extracellular vesicles. Pharmacol Rev. 2012;64(3):676–705.

14. Pegtel DM, Gould SJ, Exosomes. Annu Rev Biochem. 2019;88:487–514.
15. Théry C, Zitvogel L, Amigorena S. Exosomes: composition, biogenesis and function. Nat Rev Immunol. 2002;2(8):569–79.
16. Colombo M, Raposo G, Théry C. Biogenesis, secretion, and intercellular interactions of exosomes and other extracellular vesicles. Annu Rev Cell Dev Biol. 2014;30:255–89.
17. Kamerkar S, LeBleu VS, Sugimoto H, Yang S, Ruivo CF, Melo SA, et al. Exosomes facilitate therapeutic targeting of oncogenic KRAS in pancreatic cancer. Nature. 2017;546(7659):498–503.
18. Alvarez-Erviti L, Seow Y, Yin H, Betts C, Lakhal S, Wood MJA. Delivery of siRNA to the mouse brain by systemic injection of targeted exosomes. Nat Biotechnol. 2011;29(4):341–5.
19. Lai RC, Arslan F, Lee MM, Sze NSK, Choo A, Chen TS, et al. Exosome secreted by MSC reduces myocardial ischemia/reperfusion injury. Stem Cell Res. 2010;4(3):214–22.
20. Baglio SR, Pegtel DM, Baldini N. Mesenchymal stem cell secreted vesicles provide novel opportunities in (stem) cell-free therapy. Front Physiol. 2012;3:359.
21. Lou G, Chen Z, Zheng M, Liu Y. Mesenchymal stem cell-derived exosomes as a new therapeutic strategy for liver diseases. Exp Mol Med. 2017;49(6):e346.
22. Batrakova EV, Kim MS. Using exosomes, naturally-equipped nanocarriers, for drug delivery. J Control Release. 2015;219:396–405.
23. Ha D, Yang N, Nadithe V. Exosomes as therapeutic drug carriers and delivery vehicles across biological membranes: current perspectives and future challenges. Acta Pharm Sin B. 2016;6(4):287–96.
24. Tian Y, Li S, Song J, Ji T, Zhu M, Anderson GJ, et al. A doxorubicin delivery platform using engineered natural membrane vesicle exosomes for targeted tumor therapy. Biomaterials. 2014;35(7):2383–90.
25. Barenholz Y. Doxil® — The first FDA-approved nano-drug: Lessons learned. J Control Release. 2012;160(2):117–34.
26. Kanchanapally R, Khan MA, Deshmukh SK, Srivastava SK, Khushman M, Singh S, et al. Exosome-based synthetic nanovesicles for drug delivery in cancer. Int J Nanomed. 2019;14:531–41.
27. Freshney RI. Culture of Animal Cells: A Manual of Basic Technique and Specialized Applications. 7th ed. Hoboken, NJ: Wiley-Blackwell; 2016.
28. Théry C, Amigorena S, Raposo G, Clayton A. Isolation and characterization of exosomes from cell culture supernatants and biological fluids. Curr Protoc Cell Biol. 2006;Chap. 3:Unit 3.22.
29. Soleimani M, Nadri S. A protocol for isolation and culture of mesenchymal stem cells from mouse bone marrow. Nat Protoc. 2009;4(1):102–6.
30. Kowal J, Arras G, Colombo M, Jouve M, Morath JP, Primdal-Bengtson B, et al. Proteomic comparison defines novel markers to characterize heterogeneous populations of extracellular vesicle subtypes. Proc Natl Acad Sci U S A. 2016;113(8):E968–77.
31. Li P, Kaslan M, Lee SH, Yao J, Gao Z. Progress Exosome Isolation Techniques Theranostics. 2017;7(3):789–804.

32. Mosmann T. Rapid colorimetric assay for cellular growth and survival: application to proliferation and cytotoxicity assays. J Immunol Methods. 1983;65(1–2):55–63.
33. Vermes I, Haanen C, Steffens-Nakken H, Reutelingsperger C. A novel assay for apoptosis. Flow cytometric detection of phosphatidylserine expression on early apoptotic cells using fluorescein labelled Annexin V. J Immunol Methods. 1995;184(1):39–51.
34. Kroemer G, Galluzzi L, Vandenabeele P, Abrams J, Alnemri ES, Baehrecke EH, et al. Classification of cell death: recommendations of the Nomenclature Committee on Cell Death 2009. Cell Death Differ. 2009;16(3):3–11.
35. Ratajczak J, Wysoczynski M, Hayek F, Janowska-Wieczorek A, Ratajczak MZ. Membrane-derived microvesicles: important and underappreciated mediators of cell-to-cell communication. Leukemia. 2006;20(9):1487–95.
36. Fais S, O'Driscoll L, Borras FE, Buzas E, Camussi G, Cappello F, et al. Evidence-Based Clinical Use of Nanoscale Extracellular Vesicles in Nanomedicine. ACS Nano. 2016;10(4):3886–99.
37. Johnsen KB, Gudbergsson JM, Skov MN, Pilgaard L, Moos T, Duroux M. A comprehensive overview of exosomes as drug delivery vehicles — Endogenous nanocarriers for targeted cancer therapy. Biochim Biophys Acta. 2014;1846(1):75–87.
38. Villarroya-Beltri C, Baixauli F, Mittelbrunn M, Fernández-Delgado I, Torralba D, Moreno-Gonzalo O, et al. ISGylation controls exosome secretion by promoting lysosomal degradation of MVB proteins. Nat Commun. 2016;7:13588.
39. Sun D, Zhuang X, Xiang X, Liu Y, Zhang S, Liu C, et al. A novel nanoparticle drug delivery system: the anti-inflammatory activity of curcumin is enhanced when encapsulated in exosomes. Mol Ther. 2010;18(9):1606–14.
40. Wang T, Jian Z, Baskys A, Yang J, Li J, Guo H, et al. MSC-derived exosomes protect against oxidative stress-induced skin injury via adaptive regulation of the NRF2 defense system. Biomaterials. 2020;257:120264.
41. Raposo G, Stoorvogel W. Extracellular vesicles: exosomes, microvesicles, and friends. J Cell Biol. 2013;200(4):373–83.
42. Kowal J, Arras G, Colombo M, et al. Proteomic comparison defines novel markers to characterize extracellular vesicle subtypes. Proc Natl Acad Sci U S A. 2016;113(8):E968–77.
43. Théry C, Witwer KW, Aikawa E, et al. Minimal information for studies of extracellular vesicles 2018 (MISEV2018). J Extracell Vesicles. 2018;7(1):1535750.
44. Colombo M, Raposo G, Théry C. Biogenesis, secretion, and intercellular interactions of exosomes and other extracellular vesicles. Annu Rev Cell Dev Biol. 2014;30:255–89.
45. Raposo G, Stoorvogel W. Extracellular vesicles: exosomes, microvesicles, and friends. J Cell Biol. 2013;200(4):373–83.
46. Pegtel DM, Gould SJ, Exosomes. Annu Rev Biochem. 2019;88:487–514.

47. Pasparakis M, Vandenabeele P. Necroptosis and its role in inflammation. Nature. 2015;517(7534):311–20.
48. Kim MS, Haney MJ, Zhao Y, Mahajan V, Deygen I, Klyachko NL, et al. Development of exosome-encapsulated paclitaxel to overcome MDR in cancer cells. Nanomedicine. 2016;12(3):655–64.
49. Gabizon A, Catane R, Uziely B, Kaufman B, Safra T, Cohen R, et al. Prolonged circulation time and enhanced accumulation in malignant exudates of doxorubicin encapsulated in polyethylene-glycol coated liposomes. Cancer Res. 1994;54(4):987–92.
50. Wu M, Ouyang Y, Wang Z, Zhang R, Huang PH, Chen C, et al. Isolation of exosomes from whole blood by integrating acoustics and microfluidics. Proc Natl Acad Sci U S A. 2017;114(40):10584–9.

Figures

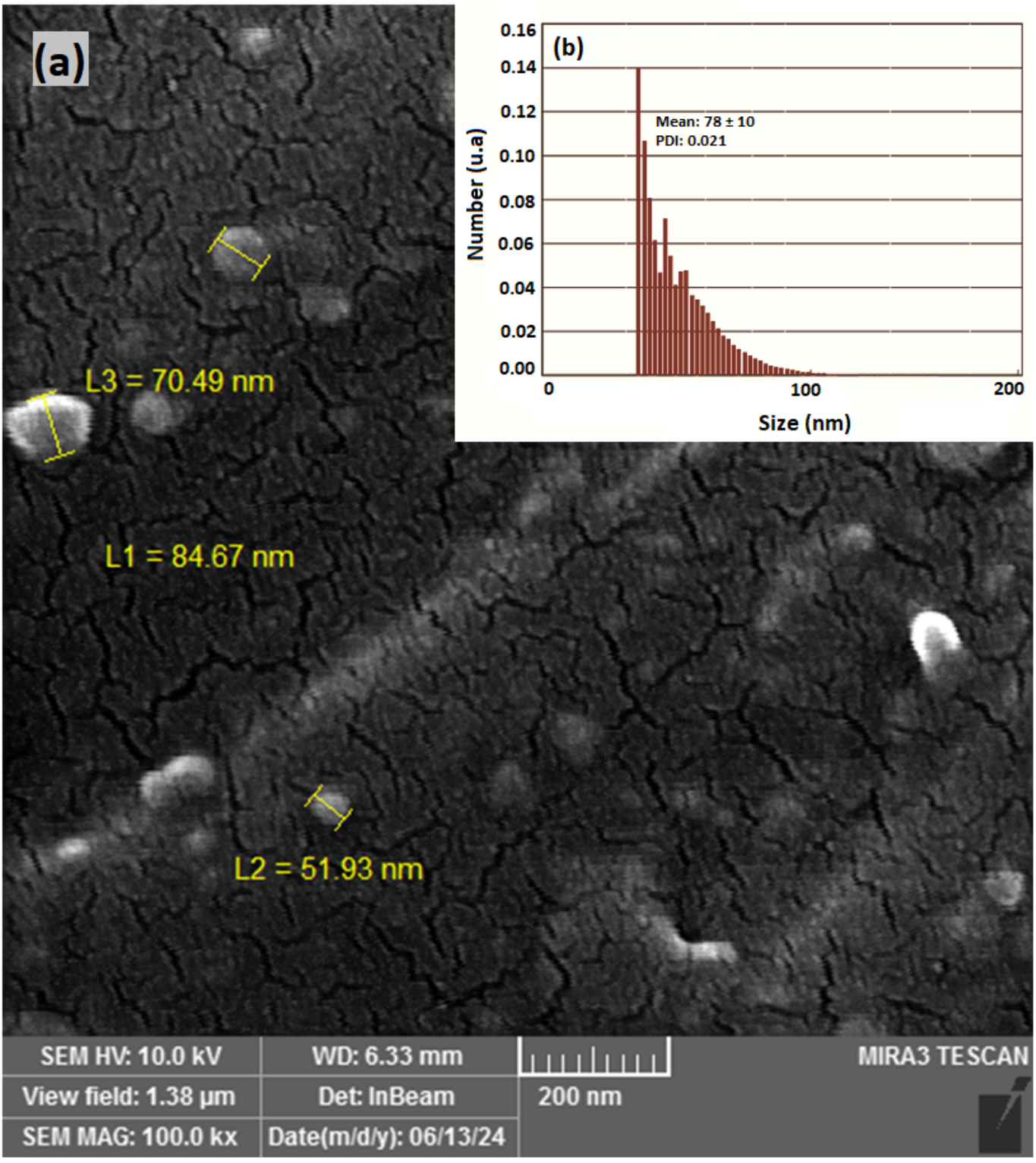


Figure 1

Physical characterization of exosome: (a) FESEM image of BM-SC derived exosome, and (b) DLS size distribution curve.

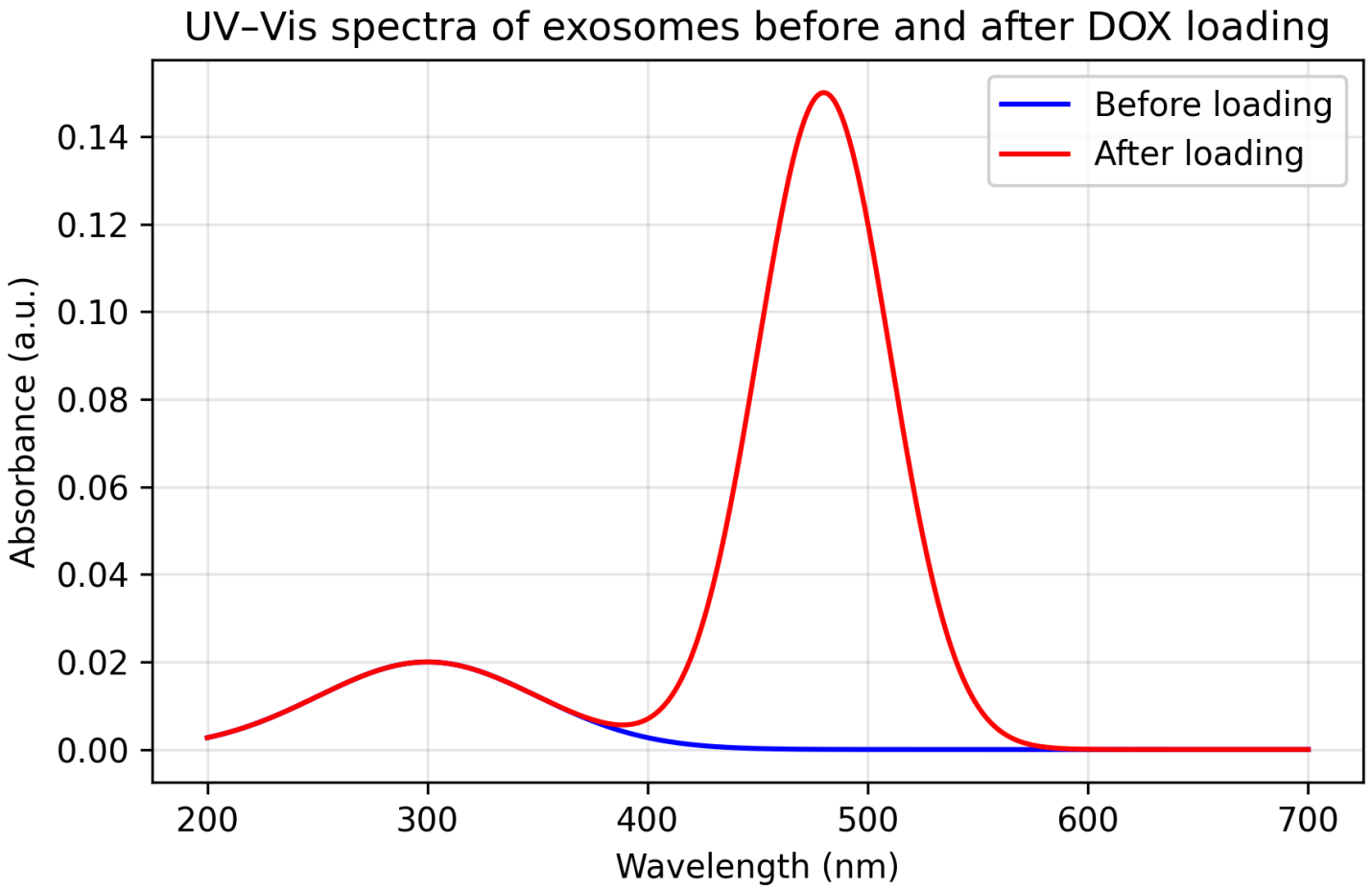


Figure 2

DOX loading workflow with UV–Vis spectra comparison before and after loading

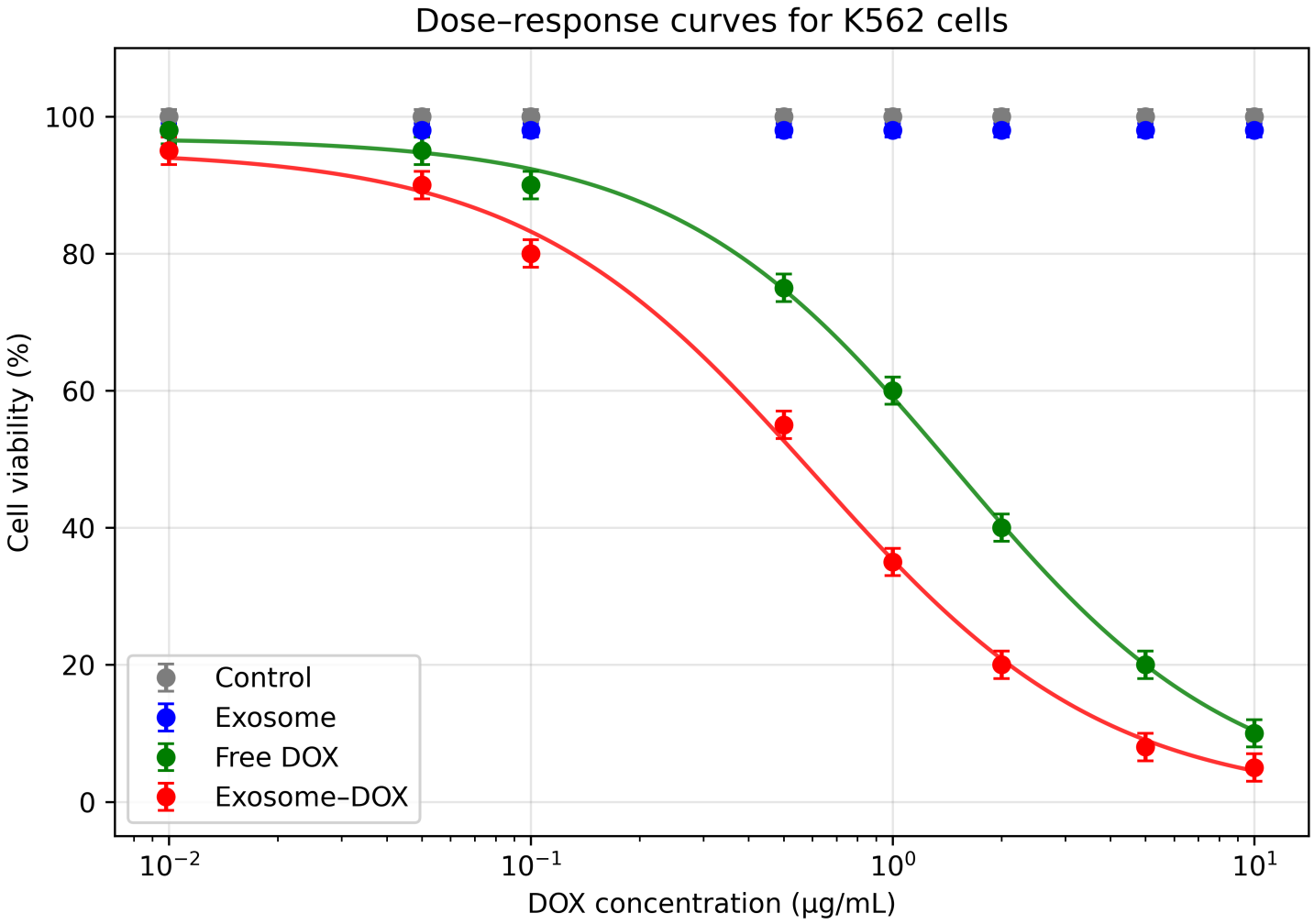


Figure 3

Dose–response cytotoxicity curves for free DOX and Exosome–DOX in K562 cells after 48 h incubation. Data represent mean ± SD (n = 3). **p**<0.05 vs free DOX.

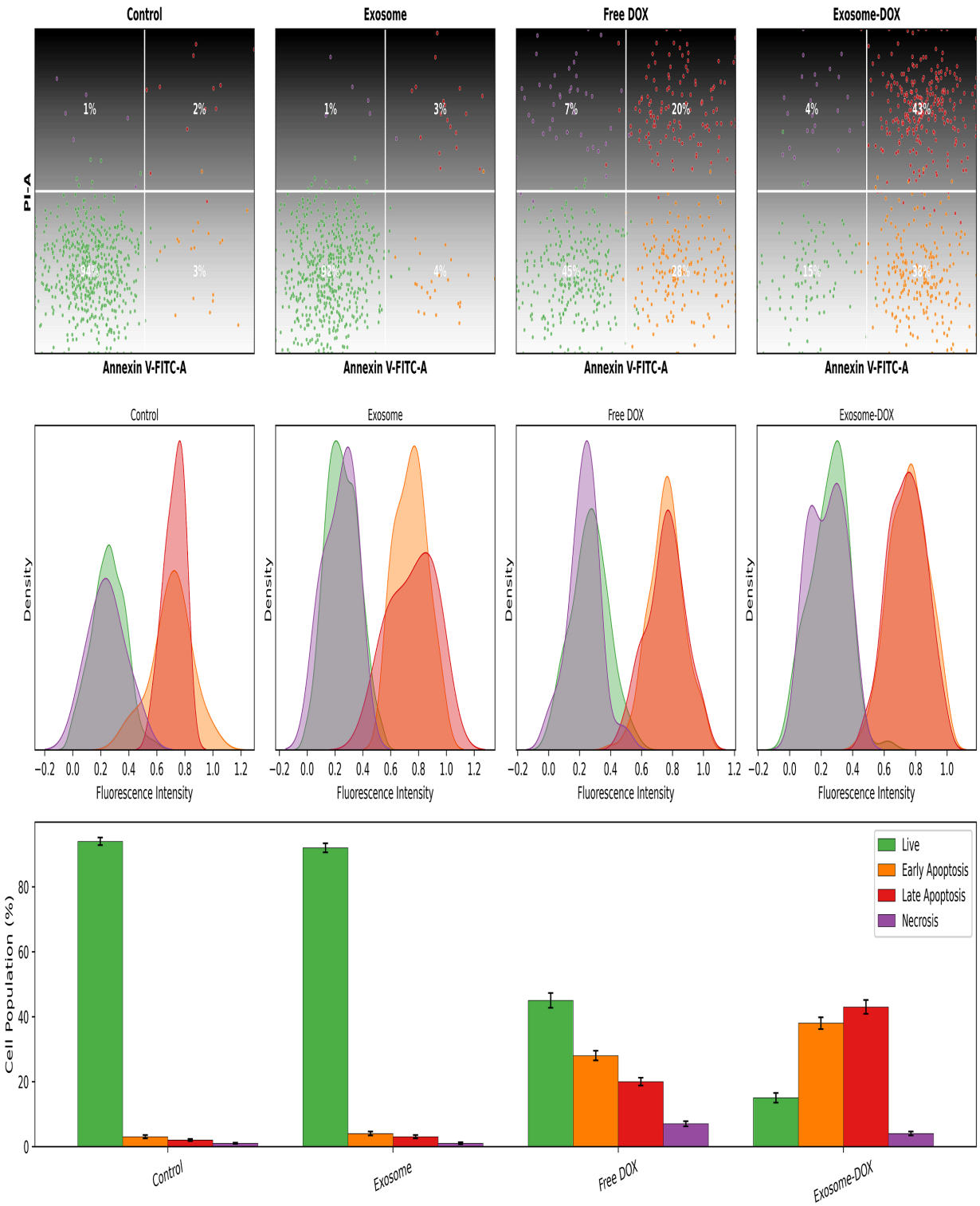


Figure 4

Flow cytometry results of (a) Representative Annexin V–FITC/PI plots for each treatment group (b) Quantitative bar graph with Mean ± SD and significance indicators (*p<0.05, **p<0.01*)

Supplementary Files

This is a list of supplementary files associated with this preprint. Click to download.

- image1.png